

Photoproduction of ω mesons on nuclei near the production threshold

M. Nanova¹, J. Weil², S. Friedrich¹, V. Metag¹, U. Mosel², M. Thiel¹, G. Anton³, J.C.S. Bacelar⁴, O. Bartholomy⁵, D. Bayadilov^{5,6}, Y.A. Beloglazov⁶, R. Bogendörfer³, R. Castelijns⁴, V. Crede^{5,a}, H. Dutz⁷, A. Ehmans⁵, D. Elsner⁷, K. Essig⁵, R. Ewald⁷, I. Fabry⁵, M. Fuchs⁵, Ch. Funke⁵, R. Gothe^{7,b}, R. Gregor¹, A.B. Gridnev⁶, E. Gutz⁵, S. Höffgen⁵, P. Hoffmeister⁵, I. Horn⁵, J. Hössl³, I. Jaegle⁸, J. Junkersfeld⁵, H. Kalinowsky⁵, Frank Klein⁷, Friedrich Klein⁷, E. Klempt⁵, M. Konrad⁷, B. Kopf^{9,10}, M. Kotulla¹, B. Krusche⁸, J. Langheinrich^{7,10}, H. Löhner⁴, I.V. Lopatin⁶, J. Lotz⁵, S. Lugert¹, D. Menze⁷, T. Mertens⁸, J.G. Messchendorp⁴, C. Morales⁷, R. Novotny¹, M. Ostrick^{7,c}, L.M. Pant^{1,d}, H. van Pee⁵, M. Pfeiffer¹, A. Roy^{1,e}, A. Radkov⁶, S. Schadmand^{1,f}, Ch. Schmidt⁵, H. Schmieden⁷, B. Schoch⁷, S. Shende^{4,h}, G. Suft³, A. Süle⁷, V. V. Sumachev⁶, T. Szczepanek⁵, U. Thoma⁵, D. Trnka¹, R. Varma^{1,g}, D. Walther⁵, Ch. Weinheimer^{5,i}, Ch. Wendel⁵
(The CBELSA/TAPS Collaboration)

¹II. Physikalisches Institut, Universität Gießen, Germany

²Inst. für Theoretische Physik I, Universität Gießen, Germany

³Physikalisches Institut, Universität Erlangen, Germany

⁴Kernfysisch Versneller Instituut Groningen, The Netherlands

⁵Helmholtz-Institut für Strahlen- u. Kernphysik Universität Bonn, Germany

⁶Petersburg Nuclear Physics Institute Gatchina, Russia

⁷Physikalisches Institut, Universität Bonn, Germany

⁸Physikalisches Institut, Universität Basel, Switzerland

⁹Institut für Kern- und Teilchenphysik TU Dresden, Germany

¹⁰Physikalisches Institut, Universität Bochum, Germany

^aCurrent address: Florida State University Tallahassee, FL, USA

^bCurrent address: University of South Carolina Columbia, SC, USA

^cCurrent address: Physikalisches Institut Universität Mainz, Germany

^dCurrent address: Nuclear Physics Division BARC, Mumbai, India

^eCurrent address: IIT Indore, Indore, India

^fCurrent address: Forschungszentrum Jülich, Germany

^gCurrent address: Department of Physics I.I.T. Powai, Mumbai, India

^hCurrent address: Department of Physics, University of Pune, Pune, India

ⁱPresent address: Universität Münster, Germany

Received: date / Revised version: date

Abstract. The photoproduction of ω mesons on LH_2 , C and Nb has been measured for incident photon energies from 900 to 1300 MeV using the CB/TAPS detector at ELSA. The ω line shape does not show any significant difference between the LH_2 and the Nb targets. The experiment was motivated by transport calculations that predicted a sensitivity of the ω line shape to in-medium modifications near the production threshold on a free nucleon of $E_\gamma^{lab} = 1109$ MeV. A comparison with recent calculations is given.

PACS. 14.40.Be Light mesons – 21.65.-f Nuclear matter – 25.20.-x Photonuclear reactions

1 Introduction

Modifications of hadron properties in a strongly interacting environment have attracted a lot of attention and have been intensively studied both theoretically and experimentally. These studies were motivated by the expect-

tation that chiral symmetry, a fundamental symmetry of Quantum Chromodynamics (QCD) in the limit of vanishing quark masses, may be restored in a nuclear medium at high temperatures or densities. In vacuum this symmetry is broken as visible in the low mass part of the hadronic spectrum: chiral partners - hadronic states with the same spin but opposite parity - like the ρ and a_1 meson are

Correspondence to: Mariana.Nanova@physik.uni-giessen.de

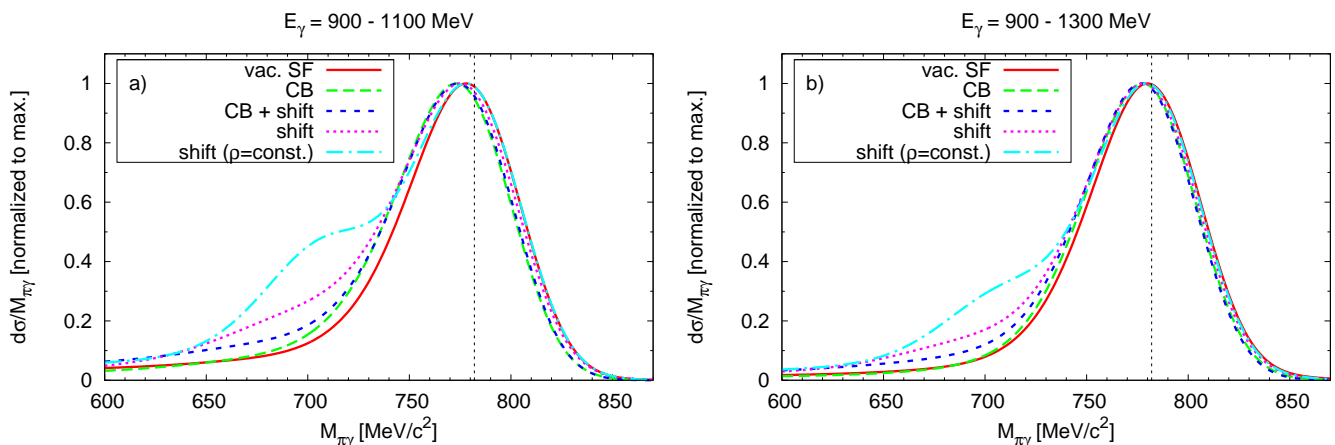


Fig. 1. (Color online) ω meson line shape predicted for a Nb target in GiBUU transport model calculations for different in-medium modification scenarios: vacuum spectral function (solid), collisional broadening of $\Gamma_{coll} = 140$ MeV (long dashed), collisional broadening and an attractive mass shift of -16% at nuclear matter density (short dashed) and mass shift without broadening (dotted). The dashed-dotted curve shows the results for a constant nuclear density of $\rho = 0.6\rho_0$. The signals are folded with the detector response given by Eq. 1 with the parameters $\sigma = 25$ MeV and $\tau = -0.09$ and take into account a $1/E_\gamma$ weighting of the bremsstrahlung spectrum. a) incident photon energies of 900 - 1100 MeV; b) incident photon energies of 900 - 1300 MeV.

different in mass while they should be mass degenerate if chiral symmetry were to hold. It turns out, however, (for details see [1]) that a connection between chiral symmetry restoration and hadronic in-medium spectral functions is much more involved. QCD sum rules provide a link between the quark-gluon sector and hadronic descriptions but do not fix the properties of hadrons in the strongly interacting medium. They only provide constraints for hadronic models which are still needed for calculating the in-medium self-energies of hadrons and their spectral functions.

Experimentally this field has been addressed in heavy ion collisions and reactions with proton and photon beams. Light vector mesons are particularly suited for these investigations since - after production in a nuclear reaction - they decay in the nuclear medium with sizable probability because of their short lifetimes. Experimental results are summarized and critically evaluated in recent reviews [1, 2]. Almost all experiments report a softening of the spectral functions of the light vector mesons ρ , ω and ϕ . Increases in width are observed depending on the density and temperature of the hadronic environment. Mass shifts are only reported by the KEK group [3, 4] who studied ρ , ω and ϕ production in proton nucleus reactions at 12 GeV. The claim of a mass shift of the ω meson in photoproduction on Nb [5] has not been confirmed in a re-analysis of the data [6].

In the latter experiment incident photon energies covered the range from 900 - 2200 MeV. Because of the increase of the production cross section with photon energy most of the observed ω mesons are produced with photons of energy larger than 1500 MeV. For the energy range of 1500 - 2200 MeV transport calculations [7, 8] have shown that the ω lineshape is rather insensitive to different in-medium modification scenarios like broadening or broad-

ening and mass shift since most of the ω decays occur outside of the nuclear medium, even despite of a cut on the ω momentum ($p_\omega \leq 500$ MeV/c). Furthermore, due to the experimentally observed strong absorption of ω mesons in the nuclear medium [9] ω mesons produced in the interior of the nucleus are largely removed by inelastic reactions and do not reach the detector; information on possible in-medium mass shifts thereby gets lost. The limited sensitivity of the ω lineshape to in-medium modifications has been confirmed experimentally in [6].

Gallmeister et al. [7] argue that a search for medium effects would be much more promising for incident photon energies below or near the photoproduction threshold on a free nucleon of $E_\gamma^{lab} = 1109$ MeV. New calculations along these lines illustrate in Fig.1 the expected sensitivity of the ω signal to various in-medium changes, such as mass shift with and without collisional broadening for two different energy ranges. It is seen that the lower-energy window indeed leads to a more pronounced - though not dramatic - sensitivity than the higher-energy one. This relatively weak sensitivity is to a large extent simply a consequence of the density profile of the nucleus that spans all densities from 0 to ρ_0 and thus smears any density-dependent signal. Assuming for the sake of the argument a density profile with a constant density of $0.6\rho_0$ - roughly corresponding to the average density in nuclei - and a sharp fall off at the surface the dash-dotted line in Fig.1 is obtained; here the in-medium signal is significantly stronger. For a realistic nuclear density profile contributions to the spectral function from the surface dominate, suppressing contributions from higher density regions [10].

In both energy windows a tail towards lower masses is predicted for the scenario of a dropping ω mass. This tail is due to ω mesons which are produced off-shell within the nucleus. In [7, 8] an even stronger enhancement in the low

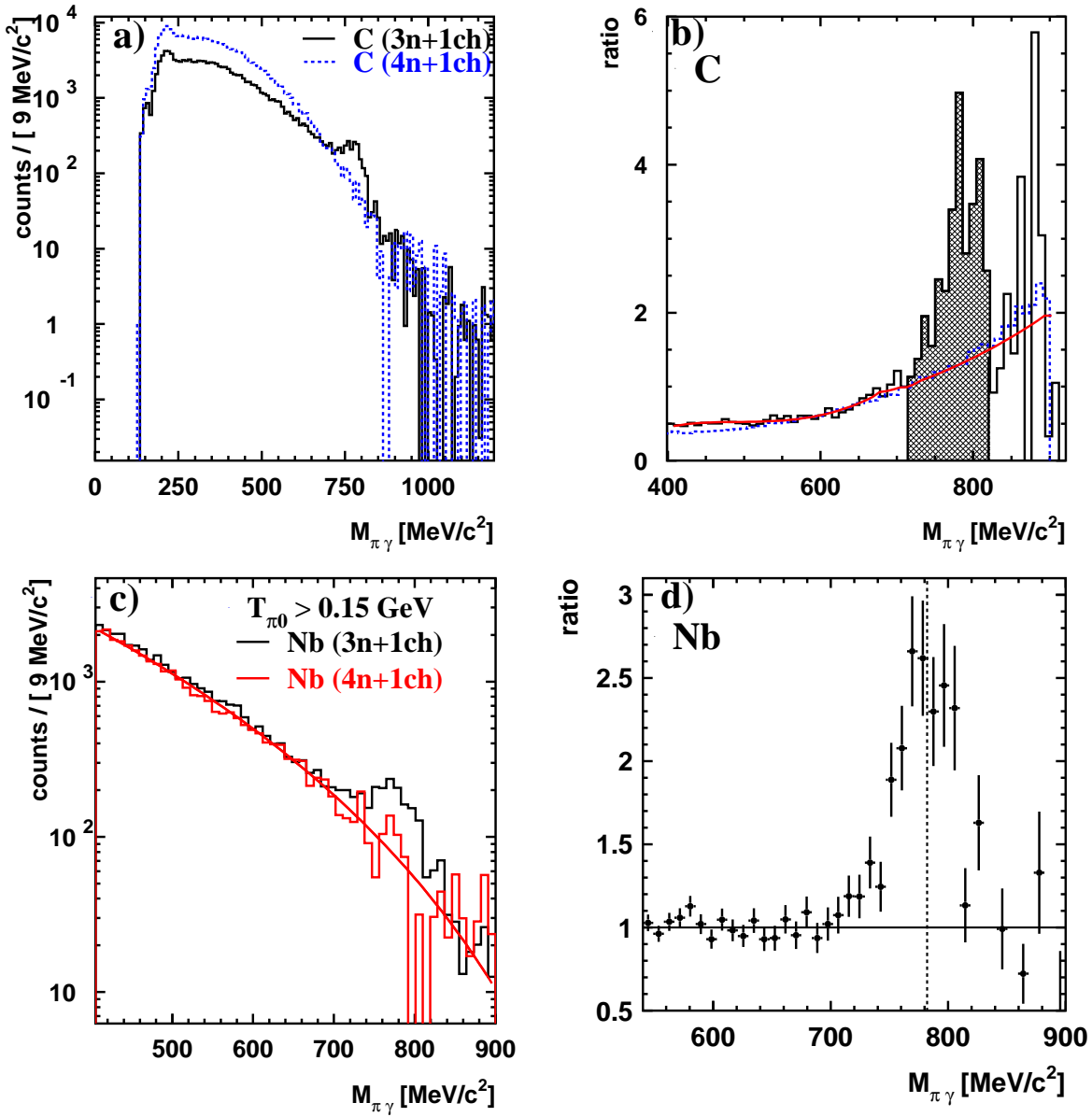


Fig. 2. (Color online) a) $\pi^0\gamma$ signal (solid curve) and background spectrum for the C target deduced from events with 4 neutral and 1 charged hit. b) Ratio of the distributions in a), reflecting the energy dependence of the probability for detecting 3 out of 4 photons relative to detecting all 4 photons per event. The red (solid) curve is a fit to the ratio ignoring the ω mass range. The blue (dashed) histogram represents a Monte Carlo simulation. c) The $\pi^0\gamma$ signal spectrum and the corrected and normalized background spectrum for the Nb target. The solid curve represents a fit to the background distribution. d) Ratio of the $\pi^0\gamma$ signal spectrum to the background spectrum for the Nb target generated from events with 4 neutral and 1 charged hit.

mass tail region was obtained. This calculation used a phenomenological method for the off-shell propagation while the present results are based on the theoretical framework provided by Leupold [11] and Juchem and Cassing [12] who have derived equations of motion for the testparticles that represent the spectral function in the transport simulation starting from the general Kadanoff-Baym equations [13]. While the Leupold and Juchem-Cassing method has a firm theoretical basis it is nevertheless useful to remember that it relies on the assumption of adiabaticity, i.e. small gradients in space and time of all physical proper-

ties (potential, density, spectral function). Non-adiabatic effects such as those at level-crossings are not taken into account.

2 Experimental set up

The experiment was performed at the ELSA electron accelerator facility [14,15] at the University of Bonn, using the Crystal Barrel/TAPS detector set up which provides an almost complete coverage of the full solid angle.

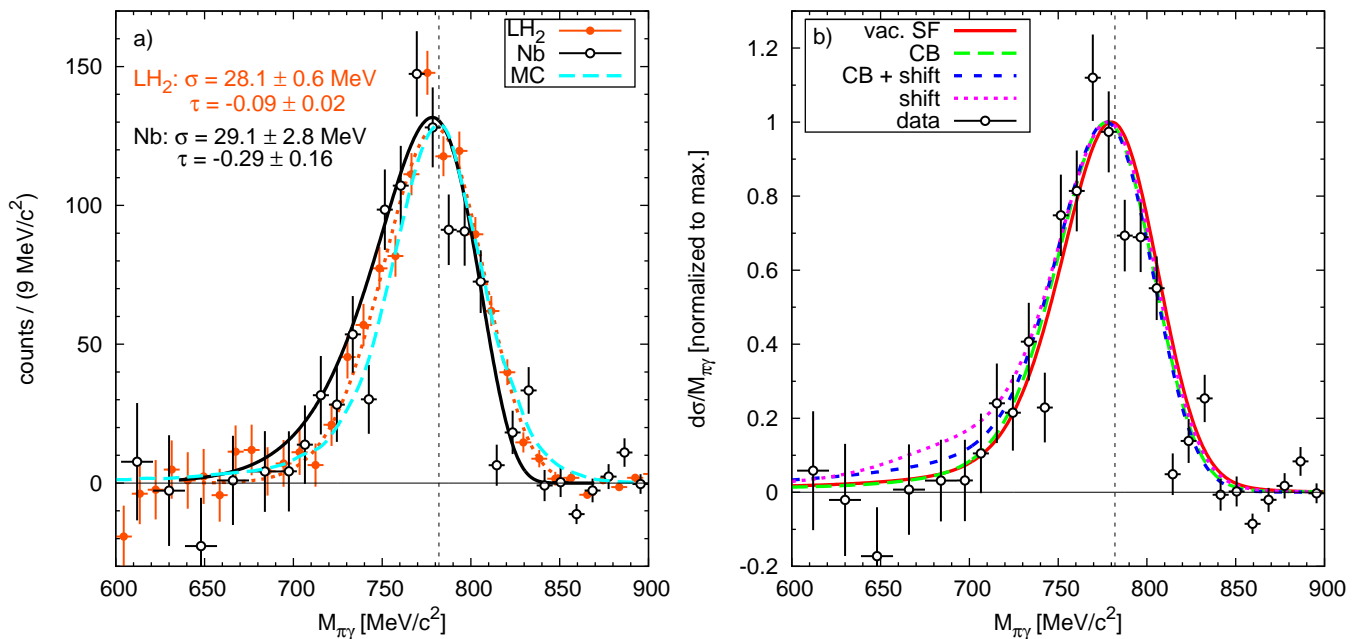


Fig. 3. (Color online) a.) ω signal (solid points) for the Nb target (1 mm thick) and incident photon energies from 900 - 1300 MeV. The errors are purely statistical. Systematic errors introduced by the background subtraction are of the order of 5% (see Fig.2b). A fit curve to the data points (see text) is shown in comparison to the ω lineshape measured on a 53 mm long LH_2 target and a Monte Carlo simulation; b.) ω signal for the Nb target in comparison to recent GiBUU simulations for the following scenarios: no medium modification (solid), in-medium broadening of $\Gamma_{coll} = 140$ MeV at nuclear saturation density (long dashed), an additional mass shift by -16% (short dashed) and mass shift without broadening (dotted). The signals are folded with with the detector response given by Eq. 1 with the parameters $\sigma = 25$ MeV and $\tau = -0.09$ and take into account a $1/E_\gamma$ weighting of the bremsstrahlung spectrum.

The features of this calorimeter system and its capability for the detection of multi-photon final states have been described in detail elsewhere [16,17,18]. Tagged photon beams of 900 - 1300 MeV were generated by bremsstrahlung and impinged in subsequent runs on LH_2 , C and Nb targets with thicknesses of 53 mm, 20 mm and 1 mm (30 mm diameter), respectively. The running conditions were the same as described in [6].

3 Analysis

The analysis of the data follows exactly the scheme described in detail in [6]. In fact, the data discussed here represent a subset of the data published in [6]. ω mesons were reconstructed in the reaction $\gamma A \rightarrow (A-1)p\omega \rightarrow (A-1)p\pi^0\gamma \rightarrow (A-1)p\gamma\gamma\gamma$ from events with 3 photons and 1 proton in the final state. Fig. 2a shows the $\pi^0\gamma$ invariant mass spectrum for the carbon target for events with 1 charged and 3 neutral hits in the system. An ω signal is observed on a steeply falling background. As discussed in [6] this background stems dominantly from $\pi^0\pi^0$ and also $\pi^0\eta \rightarrow 4\gamma$ final states where due to shower overlap in the detector or detector inefficiencies 1 out of the 4 photons escapes detection. Fig. 2a also shows the $\pi^0\gamma$ invariant mass spectrum for events with 1 charged and 4 neutral hits where 1 neutral hit has been arbitrarily omitted to simulate the background in the 3 neutral and 1

charged spectrum. The slopes of the two spectra are different, reflecting the energy dependence of the probability to register only 3 out of 4 photons relative to detecting all 4 photons. The ratio of the two spectra in Fig. 2a is given in Fig. 2b. This ratio is a smooth function of the invariant mass as verified by Monte Carlo simulations, also shown in Fig. 2b. Since no strong in-medium effects are expected for a light nucleus like carbon this ratio can be applied to correct the $\pi^0\gamma$ invariant mass spectrum derived from events with 1 charged and 4 neutral hits measured for the Nb target. Fig. 2c shows the $\pi^0\gamma$ invariant mass spectrum for Nb together with this background distribution after applying this correction. The normalization of the background spectrum is done by requesting the same number of events in the mass range from 400 - 900 MeV, excluding the counts in the ω peak which account for only 2 % of the total yield in this mass range. It is important to note that this determination of the background in magnitude and shape does not pay any attention to the ω signal region. The background in the (3 neutral +1 charged) signal spectrum is well reproduced by the corrected (4 neutral + 1 charged) spectrum. This is demonstrated by the ratio of the two spectra shown in Fig. 2d. In the mass range from 400 - 700 MeV the average deviation from unity is 5 %. This uncertainty determines the systematic error in the background subtraction.

4 Comparison to the LH_2 reference measurement and to GiBUU simulations

After subtraction of the background spectrum from the $\pi^0\gamma$ signal spectrum the ω lineshape shown in Fig. 3a is obtained for the Nb target. The experimental distribution has been fitted using the Novosibirsk function [19]:

$$f(x) = A \cdot \exp \left[-\frac{1}{2} \left(\frac{\ln q_x}{\tau} \right)^2 + \tau^2 \right] \quad (1)$$

where

$$q_x = 1 + \frac{(x - x_0)}{\sigma} \cdot \frac{\sinh(\tau\sqrt{\ln 4})}{\sqrt{\ln 4}} \quad (2)$$

Here A is the amplitude of the signal, x_0 is the peak position, σ is FWHM/2.35 and τ is the asymmetry parameter. This function takes into account the tail in the region of lower invariant masses resulting from the energy response of the calorimeters. The fit in the mass range 700 to 820 MeV is compared with the ω signal measured on the LH_2 target and with a Monte Carlo simulation of the ω signal in Fig. 3a. It should be noted that the 53 mm length of the LH_2 target leads to an increase in ω -signal width by less than 10 %. The agreement between the ω signal on the LH_2 target with the Monte Carlo simulation demonstrates that the detector response is under control. The fit parameters are $\sigma = (29.1 \pm 2.8)$ MeV, $\tau = -0.29 \pm 0.16$ for Nb and $\sigma = (28.1 \pm 0.6)$ MeV, $\tau = -0.09 \pm 0.02$ for LH_2 , respectively. The fit of the data with the function of eqs.(1),(2) yields a $\chi^2/\text{DoF} = 18.95/12$ with a χ^2 -probability of 9.0% while a fit of the data with the ω line shape measured on the LH_2 target gives a $\chi^2/\text{DoF} = 32.8/15$, corresponding to a χ^2 -probability of 0.5%. Nevertheless, in view of the systematic and statistical uncertainties no significant deviation from the reference signals is claimed. Higher statistics will be needed to draw any conclusion. Corresponding data have been taken at MAMI-C using the Crystal Ball/TAPS set up. The analysis is ongoing.

In Fig. 3b the measured ω signal is compared to predictions of transport calculations using the GiBUU model [20] for the same scenarios as in Fig. 1. While all the curves seem to underestimate the data slightly on the low mass side of the ω peak, the experimental data obviously do not allow to distinguish between the various theoretical scenarios, in contrast to initial expectations.

5 Conclusions

The photoproduction of ω mesons on LH_2 , C and Nb targets has been measured for incident photon energies from 900 - 1300 MeV, i.e. near the photoproduction threshold on a free nucleon of $E_\gamma^{lab} = 1109$ MeV. The experimentally observed ω signal does not allow to distinguish between various in-medium scenarios which - also near threshold - lead all to only a weak tail at low invariant masses. Access to the in-medium spectral function of vector mesons is thus very limited, mainly due to the dependence of the

in-medium properties such as mass and width on the nuclear density [10,21] and the inherent density-smearing caused by the density profile of nuclei. On the other hand, transparency measurements [22,23] can give at least access to the imaginary part of the in-medium self energy of the hadron. Another promising tool could be the measurement of excitation functions [24]. Such experiments are presently being analyzed.

6 Acknowledgements

We thank the scientific and technical staff at ELSA and the collaborating institutions for their important contribution to the success of the experiment. We gratefully acknowledge detailed discussions with S. Leupold and P. Mühlich. This work was supported financially by the *Deutsche Forschungs Gemeinschaft* through SFB/TR16, by the *Schweizerischer Nationalfond* and by the *Stichting voor Fundamenteel Onderzoek der Materie (FOM)* and the *Nederlandse Organisatie voor Wetenschappelijk Onderzoek (NWO)*.

References

1. S. Leupold, V. Metag and U. Mosel, Int. J. Mod. Phys. **19** No.2, (2010) 147; arXiv:0907.2388 [nucl-th].
2. R. Hayano and T. Hatsuda, arXiv:0812.1702 (2008).
3. M. Naruki et al., Phys. Rev. Lett. **96** (2006) 092301.
4. R. Muto et al., Phys. Rev. Lett. **98** (2007) 042501.
5. D. Trnka et al., Phys. Rev. Lett. **94** (2005) 192303.
6. M. Nanova et al., Phys. Rev. C **82** (2010) 035209, arXiv:1005.5694 [nucl-ex].
7. K. Gallmeister, M. Kaskulov, U. Mosel, and P. Mühlich, Prog. Part. Nucl. Phys. **61**, (2008) 283.
8. P. Mühlich, PhD thesis, Univ. of Giessen (2006).
9. M. Kotulla et al., Phys. Rev. Lett. **100** (2008) 192302.
10. U. Mosel, S. Leupold, V. Metag, arXiv:1006.5822 [nucl-th].
11. S. Leupold, Nucl. Phys. A672 (2000) 475.
12. W. Cassing and S. Juchem, Nucl. Phys. A677 (2000) 445.
13. L. P. Kadanoff and G. Baym, Quantum statistical mechanics, Benjamin, New York, 1962.
14. D. Husmann and W. J. Schuille, Phys. Bl. **44**, (1988) 40.
15. W. Hillert, Eur. Phys. J. A **28** (2006) 139.
16. E. Aker et al., Nucl. Instr. Meth. A **321** (1992) 69.
17. R. Novotny et al. IEEE Trans. Nucl. Sci. **38**, (1991) 392.
18. A. R. Gabler et al., Nucl. Instr. Meth. A **346** (1994) 168.
19. B. Aubert et al., Phys. Rev. D **70** (2004) 112006.
20. <http://gibuu.physik.uni-giessen.de>
21. J. Lehr, U. Mosel, Phys. Rev. **C64**, 042202 (2001). arXiv: 0105054 [nucl-th].
22. M. Kaskulov, E. Hernandez, and E. Oset, Eur. Phys. J. A **31**, (2007) 245.
23. P. Mühlich and U. Mosel, Nucl. Phys. A **773** (2006) 156.
24. P. Mühlich, T. Falter, U. Mosel, Eur. Phys. J. **A20**, (2004) 499, arXiv:0310067 [nucl-th].